MODELING AND DESIGN OPTIMIZATION OF A CMOS COMPATIBLE MEMS

L. Latorre [*,**], Y. Bertrand[*], P. Hazard[***], F. Pressecq[**] and P. Nouet[*]

[*] LIRMM, UMR CNRS / Université de Montpellier II, Montpellier France
[**] CNES, Quality Assurance Delegation, Toulouse, France
[***] Schneider Electric, Nanterre, France
Contact Author: P. Nouet - Phone: +33 467.41.85.27 - Fax: +33 467.41.85.00 - Email: nouet@lirmm.fr

ABSTRACT

Silicon etching at low temperature offers the possibility of manufacturing monolithic sensors with associated electronics. For a given technology, the so-called FSBM, we have established a set of relations to describe the mechanical behavior of an elementary device, the cantilever beam. We have then used these relationships for the performance evaluation and optimization of a magnetic field sensor based on the Lorentz force actuation of a « U-shape » cantilever beam.

Keywords: MEMS, Magnetic Field Sensor, Modeling, Design Optimization

INTRODUCTION

Recent advances through System-On-Chip (SOC) have led both integrated circuit designers and system providers to add more and more functions to a single Application Specific Integrated Circuit (ASIC). In that way, it appears interesting to implement a sensing element directly on the die where the electronic parts have been processed. Such approaches use low temperature post-processes to realize micrometer scale devices on a silicon substrate. An ASIC is first designed with some dedicated areas that will be post-processed in order to create sensors with dimensions of about a hundred of micrometers. A standard CMOS process is used to manufacture electronic wafers using industrial facilities thus reducing costs and enhancing yields. Then several techniques can be used to implement sensors: Front-Side Bulk Micromachining (FSBM) can be associated or not with Back-Side Bulk Micromachining (BSBM) and Sacrificial layer techniques. Extra layers can also be added to a processed wafer. As the cost of post-process is strongly affected by the needs for alignment, FSBM seems to be a very promising technique due to its self-alignment capability.

This approach generally leads to lower sensing performances compared to hybrid systems. However on-chip electronics allows better results in terms of Signal to Noise ratio and gives to the product an added-value due to on-chip calibration, offset compensation and built-in self test possibilities. Numerous physical quantities can be measured with the same technology due to its intrinsic versatility. Moreover, fabless designers can address such a technology and development costs are expected to be lower thanks to the re-use of the same technology for different physical phenomena.

FSBM TECHNOLOGY

FSBM post-process allows the fabrication of micrometric mechanical structures using a silicon wafer issued from a standard CMOS industrial process. This MEMS technology can be easily addressed in Europe through Multi-Project Wafer services of CMP [1,2]. CMOS process is either a 0.8 or 1.2 µm standard CMOS process with two metal layers from Austria Mikro Systems [3] while post-process is performed by IBS [4].

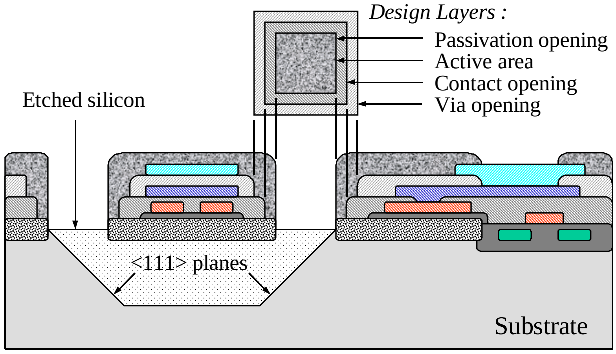

Figure 1: CMOS manufacturing process and associated post-process

Figure 1 represents a cross-sectional schematic of a CMOS process where polysilicon, metal and oxide layers are deposited on a substrate. According to designer requirements several etching masks can be superimposed to leave silicon bulk uncovered at the end of the standard CMOS process. Then, post-process operates as an anisotropic silicon etching that uses the various oxide layers as self-aligned masks. <100> substrate planes can then be etched leaving the <111> planes of silicon substrate unaltered. In that way, suspended structures can be obtained as a heterogeneous stacking of various materials (namely Silicon Oxides, Polysilicon, Aluminum, Silicon nitrides).

ELECTRO-MECHANICAL MODELING

The previously described technology allows the realization of several mechanical structures. Among them, we can list elementary devices such as cantilever beams (beam with a single clamped extremity), bridges (beam clamped at both ends) and 4-arms membranes. More complex structures can generally be described by the association of elementary ones. This section focuses on the cantilever beam as a representative device of the technology for electromechanical modeling. The complete electromechanical model will take into account the stress magnitude in polysilicon gauges. Thus, associating this stress calculation with experimental measurements of gauge resistance at calibrated forces makes possible to estimate the polysilicon gauge factor. After we described beam moment of inertia, stiffness, mass and damping, we will discuss the mechanical-to-electrical conversion using piezoresistive silicon gauges.

Heterogeneous beam model

The main difficulty of stress estimation concerns the heterogeneous composition of the beam section. Figure 2 shows a simplification method, whose principle lies in the normalization of each layer width with respect to its Young's modulus [5]. For the mechanically equivalent shape (of Young's modulus E_n), the moment of inertia I_n of the beam can be easily calculated:

$$I_n = b \times \sum \left[\frac{E_i}{E_n} \frac{t_i^3}{12} + t_i \frac{E_i}{E_n} (h_n - h_i)^2 \right] = b \times T_{In} \tag{1}$$

Where T_{In} is constant for a given technology. The position of the neutral fiber of the beam (h_n) and the vertical position of the gauge (ν_{gauge}) relatively to h_n are then geometrically deduced [6].

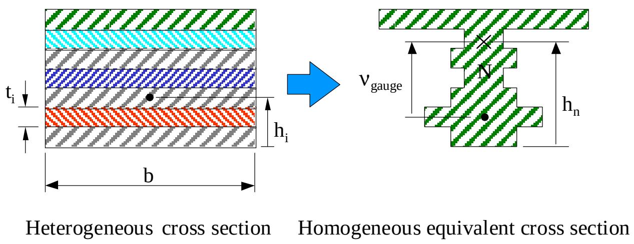

Figure 2: Normalization process of the heterogeneous section

Static behavior

According to figure 3 the stiffness k links the vertical displacement z of the beam extremity to the force F needed for creating this displacement by the following relation:

$$F = k.z \tag{2}$$

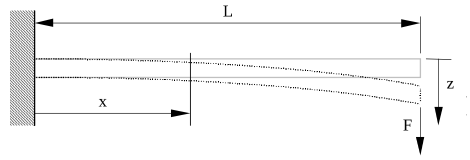

Figure 3: Stiffness modeling in a cantilever beam

The vertical displacement along the beam length *z(x)* can be deduced from the expression of the bending torque *Mf(x)* caused by the force in a second order differential equation:

$$\frac{\partial^2 z(x)}{\partial x^2} = \frac{Mf(x)}{E_n I_n} \tag{3}$$

With bending torque given by the following expression:

$$Mf(x) = F(L - x) \tag{4}$$

Finally, taking into account that the beam is clamped at $x=0$, the double integration of equation 3 gives the expression of the stiffness k:

$$z(L) = \frac{FL^3}{3E_n I_n} \quad \rightarrow \quad k = \frac{3E_n I_n}{L^3} \tag{5}$$

Dynamic behavior

The cantilever beam can be modeled by the well known second order spring–mass–damper model. The dynamic behavior is then described by the following differential equation:

$$M \frac{d^2 z(L)}{dt^2} = -k.z(L) - D\frac{dz(L)}{dt} + F \tag{6}$$

Where M is the reduced mass (at $x=L$) calculated by summing the contribution of each point of the suspended structure. Each layer mass is obtained from (i) design dimensions, (ii) data given by foundry about layers thickness and (iii) density of materials commonly found into literature [7]. In the following equation, T_M represents the mass per surface unit as a technological constant.

$$M = \frac{1}{2} T_M (b \times L) \tag{7}$$

The damping is evaluated as the damping of a plane of area $(b.L)$ and thickness Σt_i moving along z axis into air of viscosity μ_{air}.

$$D = \frac{b \times L}{\sum t_i} \mu_{air} \tag{8}$$

Force Sensing

To express the transfer function between the force input and the electrical output, we need another parameter which is the Gauge Factor. The Gauge Factor G links the relative variation of gauge resistance with both longitudinal strain ε and stress σ as:

$$G = \frac{\Delta R}{R.\varepsilon_{gauge}} = \frac{\Delta R. E_{gauge}}{R.\sigma_{gauge}} \tag{9}$$

Assuming that gauges are located at the clamped extremity of the beam to take advantage of the maximum stress, and considering the gauge length small compared to the overall length of the device, the average stress into gauge is deduced from the bending torque by:

$$\sigma_{gauge} = \frac{Mf(0)}{I_n}.\upsilon_{gauge} = \frac{F.L}{I_n}.\upsilon_{gauge} \tag{10}$$

where υ_{gauge} represents the vertical distance between the gauge and the neutral axis of the beam.

DESIGN & OPTIMIZATION

Up to now FSBM post-process has only few identified applications. The latter mostly deal with the thermal isolation obtained in a bridge (e.g. IR sensor [8]). In our approach we intend to identify mechanical applications involving deformations of microstructures. As demonstrated in the previous section, we can link an applied force with an electrical signal. For production cost reasons, all sensors involving direct application of an external force and therefore complex and expensive packaging are not considered here. Acceleration measurement is only possible in the range of 100-1000 G due to low mass of realized structures. We then focus on magnetic field sensing as magnetic field actuation has already been demonstrated for mirrors [9].

The "U-shape cantilever beam" (Figure 3) is particularly suitable for magnetic field sensing using the Lorentz force. This structure is composed with two cantilever beams linked at their free extremity by an other beam (the linking arm) in order to implement a loop. Assuming the whole device is flowed by an electrical current (the force current) and placed in a magnetic field as described in figure 4, the free length of the beam is submitted to a force. The subsequent deformation is then electrically translated thanks to strain gauges situated at the clamped end of both suspension arms. It is worth noting that the Lorentz force can be either static or dynamic depending on the nature of either magnetic field or force current.

The whole structure is mechanically equivalent to a simple cantilever beam with an equivalent width (b) equal to twice the elementary beam width (W_b). Consequently the previously described model is applicable with the following inputs:

- process parameters such as vertical dimensions (i.e. layer thickness) and piezoresistive gauge factor of polysilicon [6],
- design parameters, i.e. beam width, cantilever length (L) and width (W_c).

The design process can then be reduced to a suitable choice of those three parameters. However performance optimization will differ significantly depending on the chosen sensing mode.

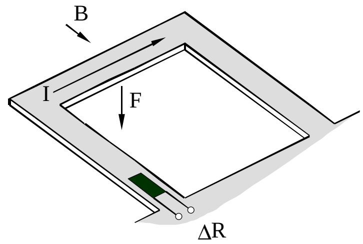

Figure 4: U-shape cantilever beam for magnetic field sensing

Design of a Static Sensor

In that case, a DC current is flowing through the beam. First of all we must establish the maximum current allowed in the beam as $I_f = d_i.W_b$ where d_i is a technological parameter giving the maximum density of current per metal width unit. The corresponding force is then $F = I_f.B.W_c = d_i.W_b.B.W_c$.

Sensor performances must be discussed in terms of both static sensitivity and bandwidth. Assuming the maximum force current is used, the static sensitivity defined as the ratio of relative variation of gauge resistance over magnetic field can be derived from equations 1, 9 and 10 to the following expression :

$$S_{stat} = \frac{G.\upsilon_{gauge}.d_i}{2.E_{gauge}.T_{In}}.L.W_C = T_1.\alpha.L^2 \tag{11}$$

where α represents the design aspect ratio of the sensor (W_C over L). As T_1 is a technological constant, the sensitivity of such a sensor is then directly linked to the silicon cost (the sensor area).

For low pass second order systems with high factor of merit, it can be considered in a first approximation that the band pass and the natural frequency are nearly equals. The latter is derived from equation 6 in its radian expression $\omega_0 = \sqrt{\frac{k}{M}}$ where the effective area taken into account for calculating both mass and damping is equal to $Wb.L(1+\alpha)$. Using also equations 1 and 5, it comes:

$$\omega_0 = \sqrt{\frac{6.T_{In}.E_n}{T_M} \times \frac{1}{L^4(1+\alpha)}} = \sqrt{T_2} \cdot \frac{1}{\mathrm{L}^2\sqrt{1+\alpha}} \tag{12}$$

where T_2 is again a technological constant.

Design of a Resonant Sensor

The dynamic resonance of a mechanical system is often used by designer to take advantage of the high figures of merit (Q) that easily reach 100 by increasing in the same amount the sensitivity. An AC current is now used to exercise the structure at its resonant frequency. The amplitude of the output signal is then modulated by the magnetic field. However for such low damped systems used as resonant sensors, the modulating signal band pass (*BP*) becomes very small. This is shown on figure 5 where a typical dynamic response of a low pass second order system is given.

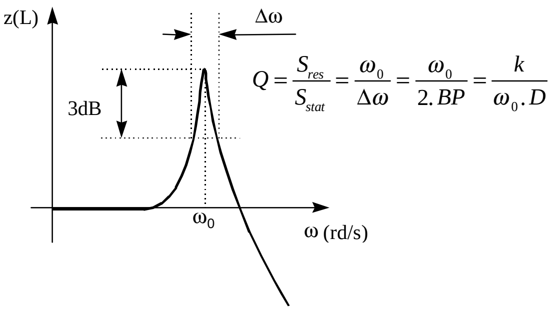

Figure 5: Dynamic response of a low-pass second order system

Using equations 1, 5, 8 and 12 we can first express the band pass of the resonant mode sensor as:

$$BP = \frac{D}{2.M} = \frac{\mu_{air}}{2.t.T_M} \qquad (13)$$

where t corresponds to the thickness of the beam (Σt_i in equation 8). It is worth noting that this equation establishes a major result for this technology: the band pass of a resonant magnetic field sensor only depends on technological parameters ($t.T_M$) and environmental conditions (μ_{air}) strongly linked to packaging constraints.

Concerning the resonant sensitivity, we use equations 1, 5, 8, 11 and 12 to deduce:

$$S_{res} = \frac{T_1 \cdot \sqrt{T_2}}{BP} \frac{\alpha}{2\sqrt{1+\alpha}} \qquad (14)$$

Once again, the resonant mode sensitivity is weakly dependent on design parameters. Only the aspect ratio of the sensor (α) influences the sensitivity in a sub-linear manner.

Overall performance

To compare the overall performance obtained in both modes, we study the product between gain and bandwidth. Concerning the resonant sensor we obtain the following expression:

$$GBW = T_1 . \sqrt{T_2} . \frac{\alpha}{2.\sqrt{1+\alpha}} \qquad (15)$$

where design parameters only influence the device through the aspect ratio of the sensor and in a sub-linear manner. For the static mode of operation, the gain-bandwidth product is twice higher.

CONCLUSION

In this paper we have introduced the analytical modeling of microstructures as an efficient alternative (or complement) to finite element modeling. For a given technology, the so-called FSBM, we have established a set of relations to describe the mechanical behavior of an elementary device, the cantilever beam. We have then used these relationships for the performance evaluation and optimization of a magnetic field sensor based on the Lorentz force actuation of a « U-shape » cantilever beam. Thanks to the analytical approach we have demonstrated that:

- static mode sensitivity is a linear function of the sensor area,
- resonant sensor bandwidth is a technological constant,
- gain-bandwidth product in the static mode is twice the resonant mode one,
- gain-bandwidth product is weakly dependent on design parameters.

An Analog HDL representation of the model has been written in order to perform simulations in a standard microelectronic CAD environment. Up to now, simulation results already remain within 10 percent of silicon data that have been obtained from a test chip [10].

References

[1] see http://tima-cmp.imag.fr/CMP/CMP.html

[2] J.M. Karam, B. Courtois, J.M. Paret, “Microelectronics Compatible Manufacturing Techniques of Microsystems”, Mechatronics ' 96.

[3] see http://www.ams.co.at

[4] Ion Beam Services, ZI Peynier Rousset, Rue Gaston Imbert Prolongée, 13790 Peynier – France – Email : ion-beam-services@wanadoo.fr

[5] S.P. Timoshenko, “Strength of Materials”, Editions D. Van Nostrand Inc., Princeton New Jersey, 1968.

[6] L. Latorre, Y. Bertrand, P. Nouet, “On the use of Test Structures for the Electromechanical characterization of a CMOS compatible MEMS technology”, Proc. IEEE ICMTS98, pp. 177-182.

[7] K. E. Petersen, “Silicon as Mechanical Material”, Proc. IEEE 1982, Vol. 70, pp. 420-457.

[8] F.V. Santos, R.A. Bianchi, J.M. Karam, B.Courtois, “CMOS Compatible IR Sensor Array”, Micromechanics Europe Conference.

[9] B.Shen, W.Allegretto, M.Hu, A.M.Robinson “CMOS Micromachined Cantilever-in-Cantilever Devices with Magnetic Actuation”, IEEE Electron Devices Letters, 1996, pp. 372-374.

[10] L. Latorre, Y. Bertrand, P. Hazard, F. Pressecq, P. Nouet, “Chararacterization and modeling of a CMOS compatible MEMS technology”, accepted for publication in Sensors & Actuators A, spring 1999.